Locating Faulty Rolling Element Bearing Signal by Simulated Annealing

Final Report

Jing Tian
Department of Mechanical Engineering
University of Maryland, College Park
jingtian@calce.umd.edu

Professor Radu Balan
Project Instructor
Department of Mathematics
University of Maryland, College Park
rvbalan@cscamm.umd.edu

Professor Kayo Ide
Project Instructor
Department of Mathematics
University of Maryland, College Park
ide@cscamm.umd.edu

Dr. Carlos Morillo
Academic Advisor
Department of Mechanical Engineering
University of Maryland, College Park
cmorillo@calce.umd.edu

Abstract

Vibration acceleration signal is widely used in the health monitoring of rolling element bearings. A critical work of the bearing fault diagnosis is locating the optimum frequency band that contains faulty bearing signal, which is usually masked by noise. This project implemented a spectral kurtosis optimization procedure to find the optimum frequency band. By performing envelope analysis to the optimum frequency band the bearing fault feature is extracted. Modules of the algorithm were validated by a combination of analytic work and simulation work. Program for the whole algorithm is evaluated by an open database of experimental data.

1. Introduction

Rolling element bearing is a mechanical element that constrains the motion and reduces the friction between two machine parts. A rolling element bearing consists of rollers, inner and outer rings, and a cage. Lubricant is applied to the contacting surfaces of the parts. Some bearings have seals to protect from dirt or contaminants.

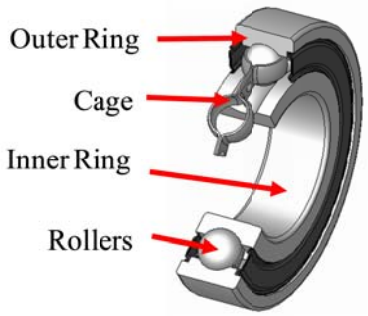

Fig. 1 Rolling element bearing
Source: http://en.wikipedia.org/wiki/Rolling-element_bearing

Rolling element bearings are widely used in different industry sectors. They are major source of system failures. In electromechanical systems, bearing faults account for more than 40% of the induction motor's failure [1], and gearbox bearing failure is the top contributor of the wind turbines downtime [2, 3]. Bearings are inexpensive devices, but the failure of bearing is costly. A $5,000 wind turbine bearing replacement can easily turn into a $250,000 project, not to mention the cost of downtime [4]. In 1987, LOT Polish Airlines Flight 5055 Il-62M crashed because of failed bearings in one engine, killing all the183 people on the plane [5]. In-situ health monitoring is used to improve the condition-based maintenance, which reduces the frequency and the loss of the bearing failure.

In the bearing health monitoring, early detection of the bearing fault is a major concern for the industry. Vibration acceleration signal is widely used in this purpose because it is sensitive to the bearing fault and it can be monitored in-situ. However, vibration signals collected by the sensor contain noise, and direct observation of the faulty bearing signal is not feasible. Therefore, the objective of the vibration signal bearing fault detection is to test if the vibration signal $x(t)$ contains the faulty bearing signal $s(t)$

$$\text{Faulty bearing:} \quad x(t) = s(t) + v(t) \tag{1}$$
$$\text{Normal bearing:} \quad x(t) = v(t) \tag{2}$$

where $x(t)$ is the monitored vibration signal; $s(t)$ is the faulty bearing signal; $v(t)$ is the noise, which is unknown.

An industrial practice to test the existence of $s(t)$ is to test if a unique frequency component of $s(t)$- the fault feature frequency component can be extracted from $x(t)$ or not. If the fault feature frequency component is extracted, the hypothesis that the bearing is faulty is true, otherwise the hypothesis is false.

According to the research in [6], faulty bearing signal $s(t)$ is a modulated signal. As a simplified representation, $s(t)$ can be expressed in the following equation:

$$s(t) = d(t)c(t) \tag{3}$$

where $d(t)$ is the modulating signal. It is a result of the periodic impact between the bearing's rolling elements and the fault on the bearing's contact surface. Its frequency component is the fault feature frequency, which is illustrated in a simulated faulty bearing signal in Fig.2. The frequency is provided by the bearing manufacturer or can be calculated from the bearing

geometry; *c(t)* is the carrier signal, which is a result of the loading and vibration transfer function. This signal is usually unknown.

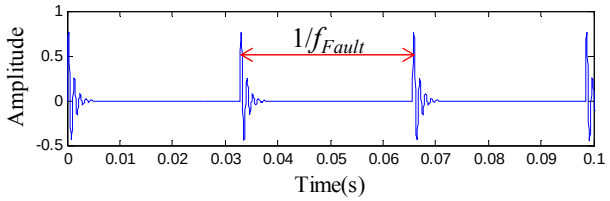

Fig. 2, Faulty bearing signal *s(t)*
f_{Fault} is the fault feature frequency

Methods like envelope analysis have been developed to extract the fault feature frequency. The problem is that in the presence of noise the extraction may fail. The solution is to band-pass filter the vibration signal in the frequency domain, as shown in a simulated vibration signal in Fig. 3.

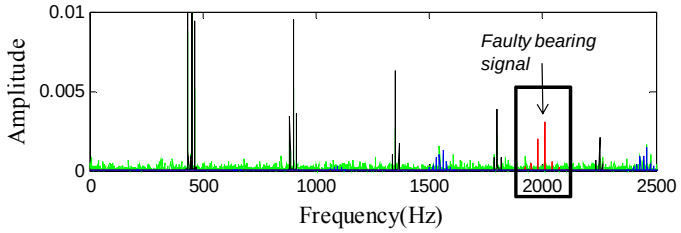

Fig. 3, Vibration signal in the frequency domain

The challenge to design the filter is that the optimum frequency band to band-pass filter the faulty bearing signal is usually unknown. This project provides a solution to find the optimum frequency band.

2. Approach for Stationary Signal

This project locates the optimum frequency band by optimizing the band-pass filter with simulated annealing (SA).

The idea is, the frequency band dominated by the faulty bearing signal is non-Gaussian, and therefore it has a high spectral kurtosis value [7]. In the presence of white Gaussian noise, by maximizing the SK, the optimum frequency band for the faulty bearing signal can be found. The optimization problem is to maximize SK in terms of the central frequency, bandwidth, and the order of the finite impulse response (FIR) band-pass filter.

$$\begin{aligned} &Maximize \quad SK(f_c, \Delta f, M) \\ &Subject \ \ to \quad f_{Fault} \le \Delta f \le \frac{f_s}{2}; \frac{\Delta f}{2} \le f_c \le \frac{f_s - \Delta f}{2} \end{aligned} \tag{4}$$

where f_c is the frequency band's central frequency; Δf is the width of the band; M is the order of FIR filter; f_{Faul} is the fault feature frequency; f_s is the sampling rate.

When the optimum frequency band is obtained, envelope analysis is applied to the filtered signal to extract the bearing faulty feature frequency.

Fig. 4 shows the flow chart of the algorithm.

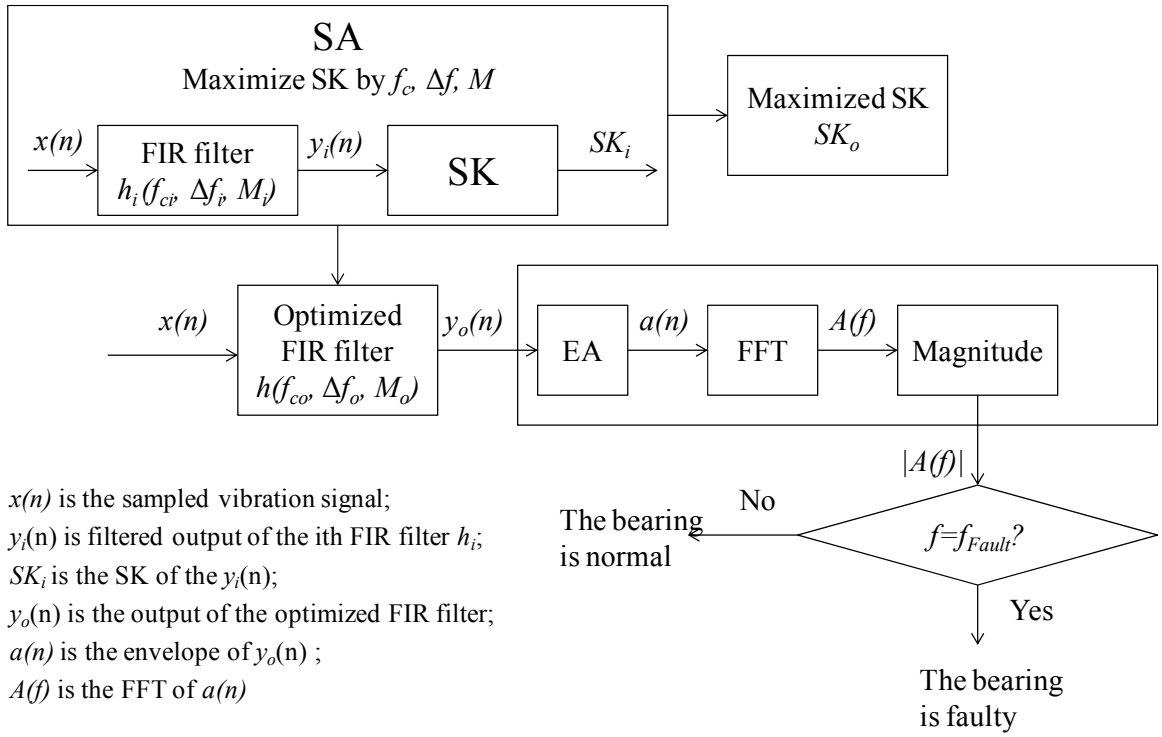

Fig. 4, Flow chart of the algorithm

2.1 Filter-bank

x(n) is the sampled version of the vibration signal *x(t)*. It has *N* points. At first, the vibration signal *x(n)* is band-pass filtered by a FIR filter *h(n)* of order M to produce the filtered signal $y=(y(n))_n$:

$$y(n) = \sum_{k=1}^{M} x(n-k)h(k) \tag{5}$$

$$h(n) = h_d(n)w(n) \tag{6}$$

$h_d(n)$ is the impulse response of the filter

$$h_d(n) = \frac{\sin[(n-M/2)\frac{f_c+\Delta f/2}{f_s/2}] - \sin[(n-M/2)\frac{f_c-\Delta f/2}{f_s/2}]}{\pi(n-M/2)} \tag{7}$$

w(n) is the window function. In this project, Hamming window will be used:

$$w(n) = 0.54 - 0.46\cos(2\pi\frac{n}{M}), 0 < n \le M \tag{8}$$

This algorithm is implemented by Matlab's build-in function "fir1".

Before optimizing the filter, initial input is obtained by calculating SK for the signal filtered by an FIR filter-bank. The filter-bank has a structure of binary tree as shown in Fig. 5. $S_{k,j}$ denotes the jth filter at the kth level. When the signal is processed by the filter-bank, sub-signals corresponding to the filters are obtained.

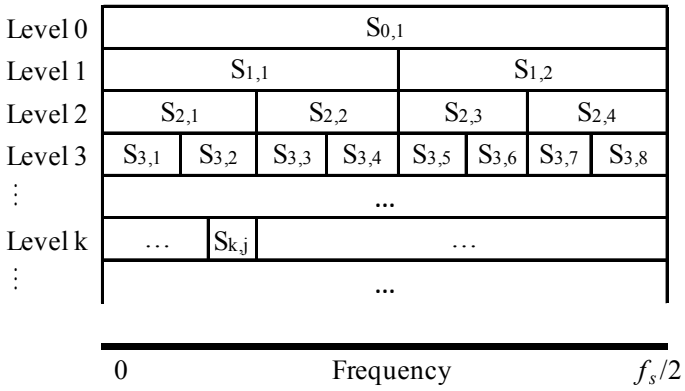

Fig. 5 Structure of the FIR filter-bank

2.2 Spectral Kurtosis

Then the spectral kurtosis of the filtered signal *y(n)* is calculated. Spectral kurtosis is defined based on the 4th order cumulants [8]:

$$SK = \frac{\kappa_4\{Y(m), Y^*(m), Y(m), Y^*(m)\}}{[\kappa_2\{Y(m), Y^*(m)\}]^2} \tag{9}$$

where κ_r is the rth order cumulant. *Y(m)* is the DFT of the signal *y(n)*:

$$Y(m) = \sum_{n=0}^{N-1} y(n) e^{-i2\pi m\frac{n}{N}}, m = 0,1,...,N-1 \tag{10}$$

Both y(n) and Y(m) are N points sequences. SK is a real number.

To estimate SK, the formula for joint cumulant is used:

$$\begin{aligned}\kappa_4\{Y(m), Y^*(m), Y(m), Y^*(m) &= E[Y(m)Y^*(m)Y(m)Y^*(m)] - E[Y(m)Y(m)] \\ &- E[Y^*(m)Y^*(m)] - 2E[Y(m)Y^*(m)]\end{aligned} \tag{11}$$

According to [9], DFT of a stationary signal is a circular complex random variable, and $E[Y(m)^2]=0$, $E[Y^*(m)^2]=0$. Therefore, we have

$$SK = \frac{E\{|Y(m)|^4\} - 2[E\{|Y(m)|^2\}]^2}{[E\{|Y(m)|^2\}]^2} = \frac{E\{|Y(m)|^4\}}{[E\{|Y(m)|^2\}]^2} - 2 \tag{12}$$

2.3 Simulated annealing

The process of estimating SK as a function of the FIR filter is optimized by simulated annealing (SA) [10], which is a metaheuristic global optimization tool. The flowchart of implementing is illustrated in Fig. 6. In reach iteration, there is a chance that a worse case would be accepted and thus simulated annealing can avoid the searching being trapped in a local minimum.

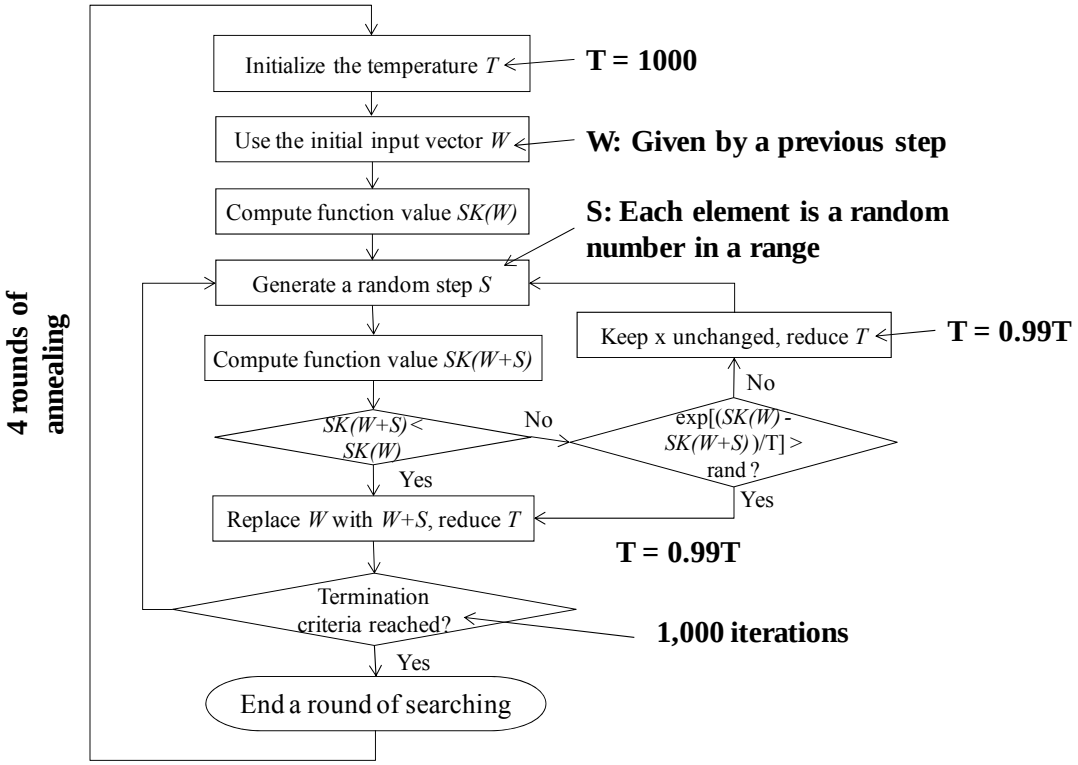

Fig. 6, Flow chart of simulated annealing

2.4 Envelope analysis

When the optimized frequency band is found, envelope analysis is applied to the filtered signal. The enveloped signal is obtained from the magnitude of the analytic signal which is constructed via Hilbert transform:

$$\hat{y}_o(t) = \int_{-\infty}^{\infty} y_o(\tau) h(t-\tau) d\tau \tag{13}$$

$$h(t) = \frac{1}{\pi t} \tag{14}$$

Analytic signal

$$y_a(t) = y_o(t) + j\hat{y}_o(t) \tag{15}$$

The envelope is the magnitude of the analytic signal

$$a(t) = | y_a(t) | \tag{16}$$

Fig. 7 shows the effect of envelope analysis on a modulated signal

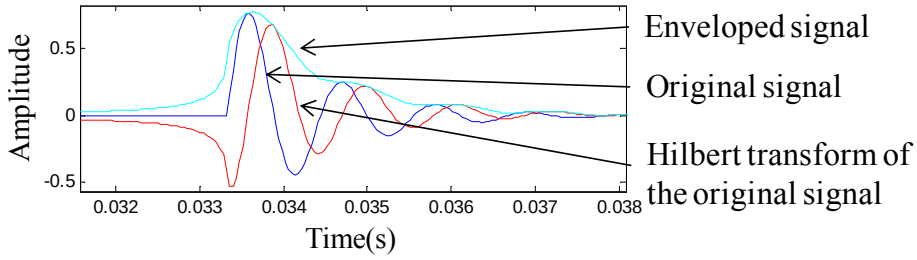

Fig. 7, Effect of envelope analysis

3. Approach for non-stationary signal

SK estimated from equation (12) requires that the signal must be stationary. In some literatures the faulty bearing signals were treated as stationary, but according to [11] the faulty bearing signal has small random variation in its frequency, thus the signal may not be truly stationary. In this approach a new definition of SK for non-stationary signal is used.

3.1 SK for non-stationary signal

In the new definition SK is estimated based on short-time Fourier transform (STFT), which is expressed in equation (17) [7]:

$$K(m) = \frac{\left\langle | X(n,m) |^4 \right\rangle}{\left\langle | X(n,m) |^2 \right\rangle^2} \tag{17}$$

where *K(m)* is the spectral kurtosis around the frequency *m*; *X(n,m)* is the STFT of the raw signal $x=(x(k))_k$. Y(n,m)=| *X(n,m)*| is the magnitude of *X(n,m)*. *n* is the time index and *m* is the frequency index. 〈•〉 is the time averaging operator that

$$\left\langle f(k) \right\rangle = \frac{1}{T} \sum_{k=1}^{T} f(k) \tag{18}$$

STFT of the signal *x(n)* is:

$$X(n,m) = \sum_{k=0}^{N-1} x(k) w(k-n) e^{-j 2\pi m / f_s} \tag{19}$$

f_s is the sampling rate; *w* is the window function. In this project, Hanning window is used, which is:

$$w(n) = 0.5(1 - \cos(\frac{2\pi n}{N-1})) \tag{20}$$

3.2 Algorithm for the new approach

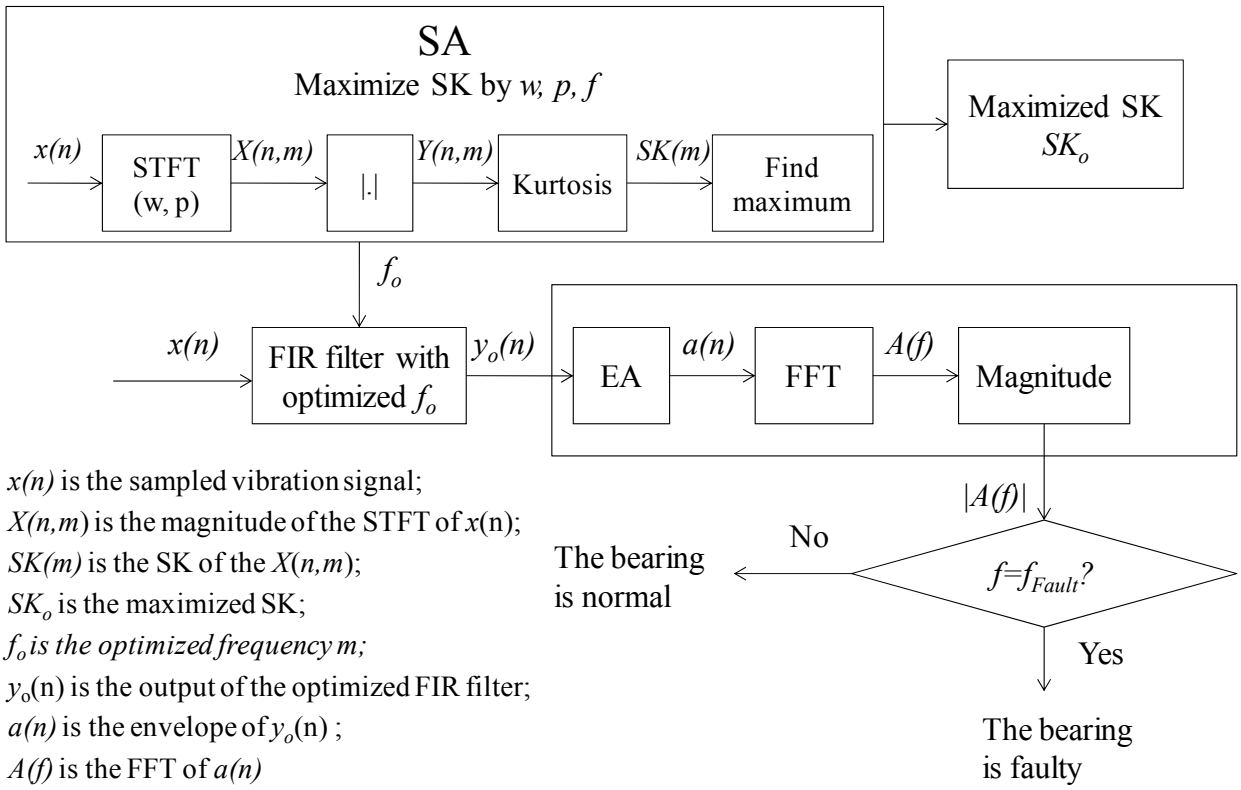

Fig. 8, Flow chart of the algorithm of the new approach

4. Validation

4.1 Validation by simulated data

An accepted bearing vibration signal generation model was developed in [6], as expressed in equation (21):

$$s(t) = d_0 a_0 q_0 \sum_{k=0}^{N} \underbrace{\left[\delta\left(t - kT_o\right)\right.}_{\text{Impulse series}} \underbrace{\sin\left(2\pi f_n\left(t - kT_o\right)\right)}_{\text{Resonance}} \underbrace{\left.e^{-\xi\left(t-kT_o\right)}\right]}_{\text{Decay}} \tag{21}$$

This model contains three parts that correspond to the physical mechanism. The first part is the impulse series generated by the impact of the rolling elements and the fault; the second part is the resonance excited by the impact; the third part is the decay of each impulse.

To generate the signal, parameters were set as d_0=1; a_0=100; q_0=1; f_n=3000 (the carrier frequency); T_0=1/100 (reciprocal of the modulating frequency).

Gaussian white noise v(n) is added to the signal, and the SNR is 8. The noise corrupted signal is illustrated in Fig. 9.

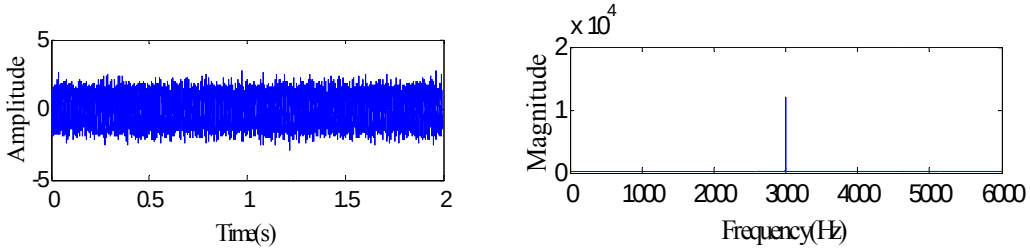

Fig. 9, Simulated signal (left: time series; right: frequency domain)

The designed optimum frequency band is: central frequency f_c=3000Hz; bandwidth f_d=100Hz. The modulating frequency to be extracted is 100Hz.

In the implementation of approach 1 for the simulated data, start point of the simulated annealing found by the algorithm was f_c=3188Hz, f_d=375Hz, filter order M=1024, and spectral kurtosis SK=8314. After optimization, the optimized filter is f_c=3165Hz; f_d=374Hz, M=975and the maximized SK=10573.

After performing envelope analysis to the optimized frequency band, the modulating frequency component was extracted, as shown in Fig. 10.

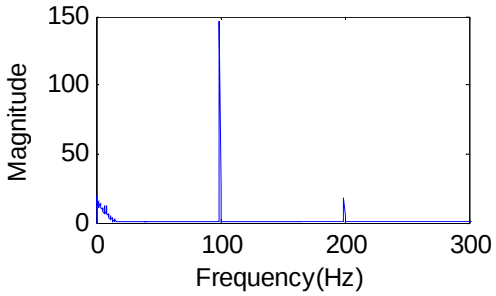

Fig. 10, Magnitude of the FFT of the demodulated signal.

4.2 Validation by experimental data

The experimental data used in this experiment is from a database [12] which is open to public by Case Western Reserve University.

The data was generated by a test rig where an accelerometer collected data from a faulty bearing driven by a motor, as shown in Fig. 11.

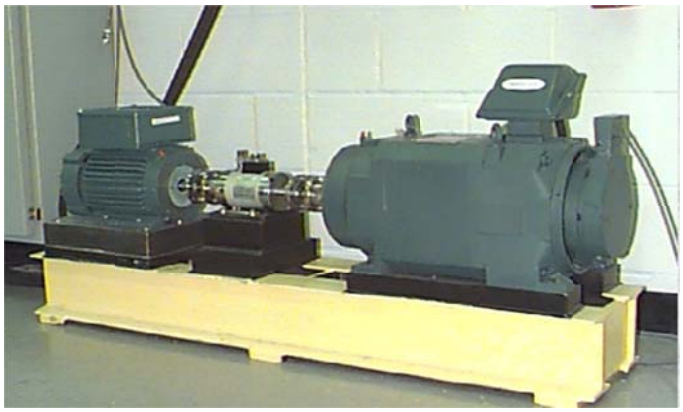

Fig. 11, Test rig reproduced from [12]

12 sets of "Fan-End Bearing Fault Data, Inner Race" from [12] were used to validate the algorithm. In all the 12 sets of data, bearings have fault on inner race fault. The sampling rate is 12,000Hz. 24,000 data points of each set were used in this project.

Time series and magnitude of the FFT for the experiment data set (No. 281) is shown below in Fig. 12.

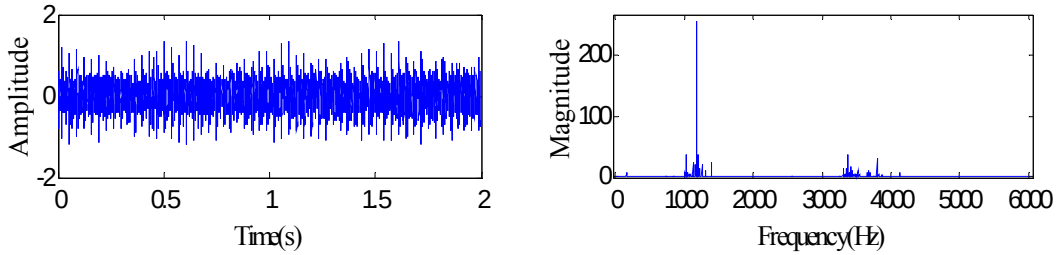

Fig. 12, One set of experimental data

By applying the algorithm of the first approach, following results were obtained. The red dash line indicate the expected fault feature frequency. Obviously, this approach does not work well for the experimental data.

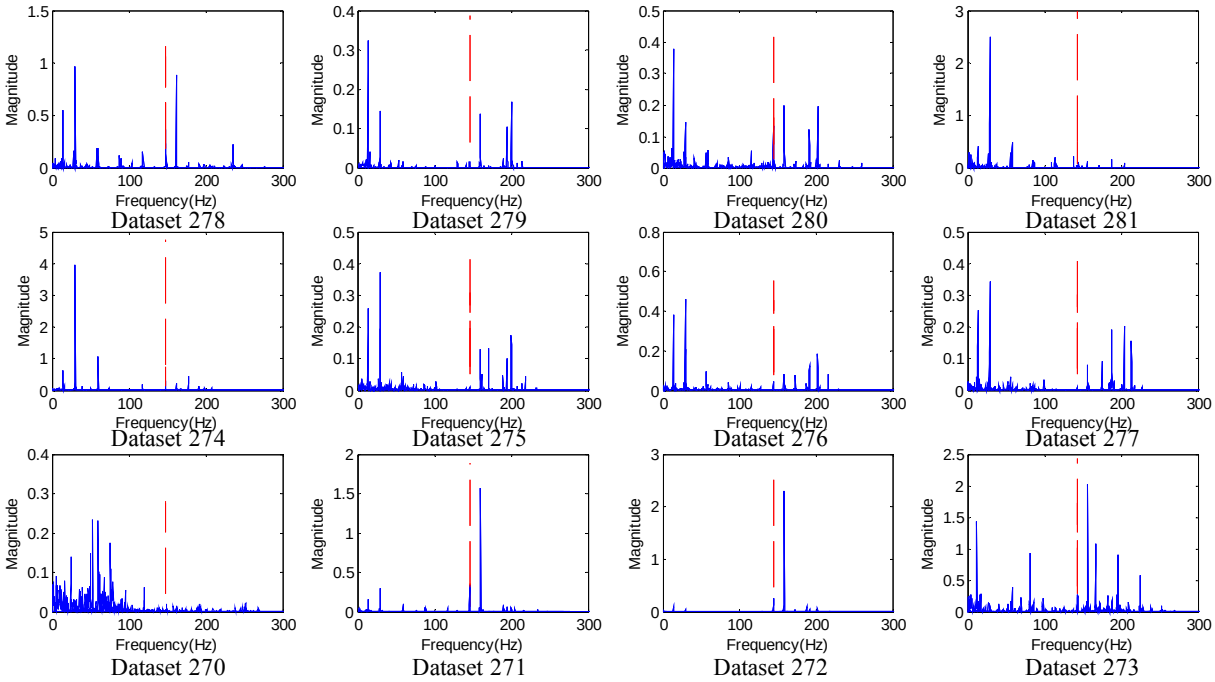

Fig. 13, Results for the experimental data of the first approach

Since the SK defined in the first approach is valid only for stationary signal, and the bearing signal may be non-stationary, so the algorithm of the second approach, which is based on SK defined for non-stationary data, should improve the result. Fig. 14 shows the analysis result of the second approach.

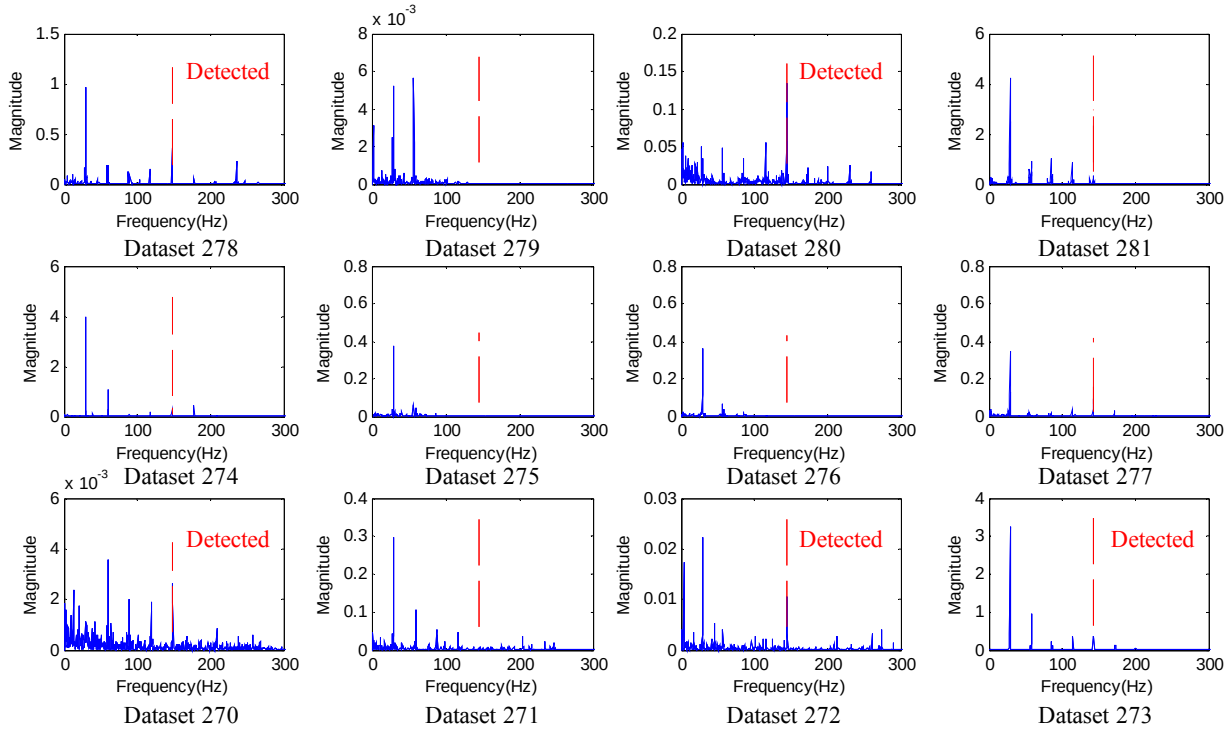

Fig. 14, Results for the experimental data of the second approach

As expected, the second approach improves the result for experimental data. But fault features were not extracted for more than half of the data sets.

5. Parallel Computing

In the optimization step, because multiple rounds of annealing can be carried out independently, parallel computing can be implemented to improve the computing efficiency. In this project, parallelization has been implemented in the second approach as shown in Fig. 15.

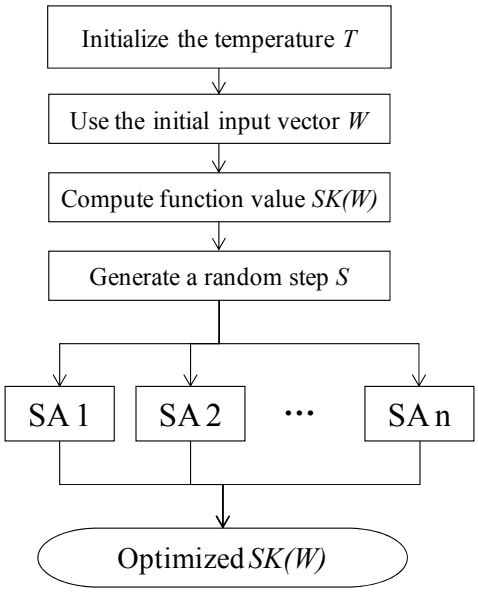

Fig. 15, Flowchart for parallelization

Multi-core computing is used to implement parallelization. Matlab "parfor" command was used in this project. 4 rounds of simulated annealing were run in parallel. At the end of optimization, the best result of the 4 rounds was used as the output.

The algorithm was run on a computer with Intel Core Duo CPU E7500 2.93GHz and 2.00GB memory, which is similar to bearing online monitoring computers.

Analysis result for the experimental data is shown in Fig. 16.

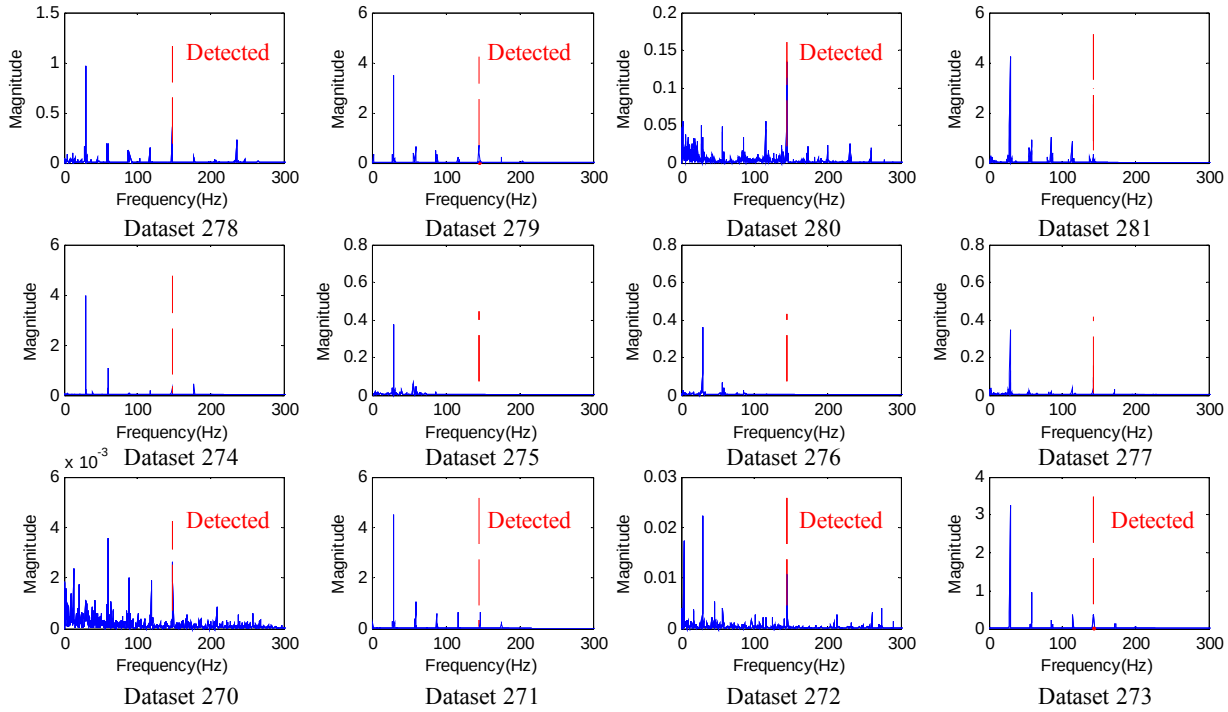

Fig. 16, Results of parallel computing

Except for the data set 279 and 271, results for serial computing and parallel computing are the same. Table I. compares the results. Yes = detected; No = not detected

Table I. Comparison of serial and parallel computing results

Data set	278	279	280	281	274	275	276	277	270	271	272	273
Serial	Yes	No	Yes	No	No	No	No	No	Yes	No	Yes	Yes
Parallel	Yes	Yes	Yes	No	No	No	No	No	Yes	Yes	Yes	Yes

Executing time of serial computing and parallel computing is compared in Table II. Overhead is not included in the calculation of time. For the given hardware, parallel computing does not improve the efficiency of computation.

Table I. Comparison of computing time

6. Conclusions

In this project a bearing fault feature extraction algorithm is developed. While spectral kurtosis is capable to evaluate the bearing fault information carried in a frequency band, simulated annealing enables spectral kurtosis to search a large range of frequency bands thus the frequency band contains most of the fault information can be located.

In this project the experimental data is difficult to be fit with a model for further evaluation, and simulated annealing provides a solution to perform optimization tasks for this data. It is also observed that the spectral kurtosis estimated as the kurtosis of the raw signal's Fourier transform can extract correct information from simulated stationary signal, but it does not work for experimental data, which is likely to be non-stationary. On the other hand, the spectral kurtosis estimated based on short-time Fourier transform is more suitable to process the experimental data. Finally, parallel computation can be applied to the re-annealing stage in simulated annealing. However, depending on the hardware, the efficiency of computation may not necessarily be improved.

Acknowledgements

I would like to thank Prof. Radu Balan and Prof. Kayo Ide for their insightful guidance and patients with me. I would also like to thank Dr. Carlos Morillo for his guidance and encouragement.

References

[1] L. M. Popa, B.-B. Jensen, E. Ritchie, and I. Boldea, “Condition monitoring of wind generators,” in *Proc. IAS Annu. Meeting*, vol. 3, 2003, pp. 1839-1846.

[2] Wind Stats Newsletter, 2003–2009, vol. 16, no. 1 to vol. 22, no. 4, Haymarket Business Media, London, UK.

[3] H. Link; W. LaCava, J. van Dam, B. McNiff, S. Sheng, R. Wallen, M. McDade, S. Lambert, S. Butterfield, and F. Oyague,“Gearbox reliability collaborative project report: findings from Phase 1 and Phase 2 testing", NREL Report No. TP-5000-51885, 2011.

[4] C. Hatch, “Improved wind turbine condition monitoring using acceleration enveloping,” Orbit, pp. 58-61, 2004.

[5] Plane crash information
http://www.planecrashinfo.com/1987/1987-26.htm

[6] P. D. Mcfadden, and J. D. Smith, “Model for the vibration produced by a single point defect in a rolling element bearing,” Journal of Sound and Vibration, 96, pp. 69-82, 1984.

[7] J. Antoni, “The spectral kurtosis: a useful tool for characterising non-stationary signals”, *Mechanical Systems and Signal Processing*, **20,** pp.282-307, 2006.

[8] V. D. Vrabie, P. Granjon, and C. Serviere, “Spectral kurtosis: from definition to application,” 6th IEEE International Workshop on Nonlinear Signal and Image Processing (NSIP 2003), Grado Trieste: Italy, 2003.

[9] P. O. Amblard, M. Gaeta, J. L. Lacoume, “Statistics for complex variables and signals - Part I: Variables”, Signal Processing **53**, pp. 1-13, 1996.
[10] S. Kirkpatrick, C. D. Gelatt, and M. P. Vecchi, "Optimization by Simulated Annealing". *Science* **220** (4598), pp. 671–680, 1983.
[11] R. B. Randall, and J. Antoni, “Rolling element bearing diagnostics—A tutorial,” Mechanical Systems and Signal Processing, **25** (2), pp.485-520, 2011.
[12] Case Western Reserve University Bearing Data Center
http://csegroups.case.edu/bearingdatacenter/home